

REPORT DOCUMENTATION PAGE				Form Approved OMB No. 0704-0188	
Public reporting burden for this collection of information is estimated to average 1 hour per response, including the time for reviewing instructions, searching existing data sources, gathering and maintaining the data needed, and completing and reviewing this collection of information. Send comments regarding this burden estimate or any other aspect of this collection of information, including suggestions for reducing this burden to Department of Defense, Washington Headquarters Services, Directorate for Information Operations and Reports (0704-0188), 1215 Jefferson Davis Highway, Suite 1204, Arlington, VA 22202-4302. Respondents should be aware that notwithstanding any other provision of law, no person shall be subject to any penalty for failing to comply with a collection of information if it does not display a currently valid OMB control number. <b>PLEASE DO NOT RETURN YOUR FORM TO THE ABOVE ADDRESS.</b>					
1. REPORT DATE (DD-MM-YYYY) 18-01-2006		2. REPORT TYPE Journal Article		3. DATES COVERED (From - To)	
4. TITLE AND SUBTITLE  Electronic Structure Studies of High Energy Ionic Liquids (Preprint)				5a. CONTRACT NUMBER	
				5b. GRANT NUMBER	
				5c. PROGRAM ELEMENT NUMBER	
6. AUTHOR(S) Deborah D. Zorn & Mark S. Gordon (Iowa State Univ.); Jerry A. Boatz (AFRL/PRSP)				5d. PROJECT NUMBER 23030423	
				5e. TASK NUMBER	
				5f. WORK UNIT NUMBER	
7. PERFORMING ORGANIZATION NAME(S) AND ADDRESS(ES)  Air Force Research Laboratory (AFMC) AFRL/PRSP 10 E. Saturn Boulevard Edwards AFB CA 93524-7680				8. PERFORMING ORGANIZATION REPORT NUMBER  AFRL-PR-ED-JA-2006-017	
9. SPONSORING / MONITORING AGENCY NAME(S) AND ADDRESS(ES)  Air Force Research Laboratory (AFMC) AFRL/PRS 5 Pollux Drive Edwards AFB CA 93524-7048				10. SPONSOR/MONITOR'S ACRONYM(S)	
				11. SPONSOR/MONITOR'S NUMBER(S) AFRL-PR-ED-JA-2006-017	
12. DISTRIBUTION / AVAILABILITY STATEMENT  Approved for public release; distribution unlimited (AFRL-ERS-PAS-2006-017)					
13. SUPPLEMENTARY NOTES Submitted for publication in Journal of Physical Chemistry					
14. ABSTRACT New energetic ionic liquids are investigated as potential high energy density materials. Ionic liquids are composed of large, charge-diffuse cations, coupled with various (usually oxygen containing) anions. In this work, calculations have been performed on the tetrazolium cation with a variety of substituents. Density functional theory (DFT) with the B3LYP functional, using the 6-311G(d,p) basis set was used to optimize geometries. Improved treatment of dynamic electron correlation was obtained using second order perturbation theory (MP2). Heats of formation of the cation with different substituent groups were calculated using isodesmic reactions and Gaussian-2 calculations on the reactants. The cation was paired with oxygen rich anions ClO <sub>4</sub> <sup>-</sup> , NO <sub>3</sub> <sup>-</sup> , or N(NO <sub>2</sub> ) <sub>2</sub> <sup>-</sup> and those structures were optimized using both DFT and MP2. The reaction pathway for proton transfer from the cation to the anion was investigated.					
15. SUBJECT TERMS					
16. SECURITY CLASSIFICATION OF:			17. LIMITATION OF ABSTRACT  A	18. NUMBER OF PAGES  37	19a. NAME OF RESPONSIBLE PERSON Dr. Scott A. Shackelford
a. REPORT Unclassified	b. ABSTRACT Unclassified	c. THIS PAGE Unclassified			19b. TELEPHONE NUMBER (include area code) N/A

## **Electronic Structure Studies of High Energy Ionic Liquids (Preprint)**

Deborah D. Zorn<sup>1</sup> Jerry A. Boatz<sup>2</sup> and Mark S. Gordon<sup>1</sup>,

<sup>1</sup>Department of Chemistry, Iowa State University, Ames, IA 50011

<sup>2</sup>Air Force Research Laboratory, Propulsion Sciences and Advanced Concepts Division,  
AFRL/PRS, 10 E. Saturn Blvd., Edward AFB, CA 93524

### **Abstract:**

New energetic ionic liquids are investigated as potential high energy density materials. Ionic liquids are composed of large, charge-diffuse cations, coupled with various (usually oxygen containing) anions. In this work, calculations have been performed on the tetrazolium cation with a variety of substituents. Density functional theory (DFT) with the B3LYP functional, using the 6-311G(d,p) basis set was used to optimize geometries. Improved treatment of dynamic electron correlation was obtained using second order perturbation theory (MP2). Heats of formation of the cation with different substituent groups were calculated using isodesmic reactions and Gaussian-2 calculations on the reactants. The cation was paired with oxygen rich anions  $\text{ClO}_4^-$ ,  $\text{NO}_3^-$ , or  $\text{N}(\text{NO}_2)_2^-$  and those structures were optimized using both DFT and MP2. The reaction pathway for proton transfer from the cation to the anion was investigated.

## Introduction

There is considerable current interest in ionic liquids as solvents. No other class of solvents offers the versatility that ionic liquids do: They are typically thermally stable, have negligibly low vapor pressure, high density, and large liquid ranges up to 400°C. Because of these unique properties, ionic liquids may be used as electrolytes for batteries, extraction media, and catalyst carriers. The popularity of ionic liquids has also been spurred on by their classification as 'green,' due to their negligible vapor pressure, thereby decreasing levels of volatile organic carbons in the environment [1].

1-Butyl-3-methyl-imidazolium (BMIM) is one of the most widely used and best understood ionic liquid cations, so when beginning to design energetic ionic liquids, this cation is a natural place to start. The unsubstituted imidazolium cation is shown in Figure 1a. The energy content of the ionic liquid cation needs to be raised for high energy applications, and this can be done in several ways.

First, replacing the imidazolium ring with a more nitrogen rich ring can increase the energy content of the ionic liquid. Second, the hydrogen or alkyl side chains can be replaced with high energy groups, such as -CN, -NH<sub>2</sub>, -N<sub>3</sub>, and -NO<sub>2</sub>. Finally, the anion chosen should be oxygen rich to serve as an oxidizer. Interesting anions include nitrate, perchlorate, and dinitramide anions (Figure 2). Two promising nitrogen-rich candidates are the triazolium (Figure 1b) and the tetrazolium (Figure 1c) cations with three and four nitrogens respectively, in the ring. These two cations could present a useful balance between endothermicity and thermal stability. A thorough study of the 1,2,4-triazolium cation has recently been published [2]. The focus of the present study is on the electronic structure of the tetrazolium cation.

The energetic tetrazolium cations that have been synthesized include 1-amino-4,5-dimethyltetrazolium [3], 2-amino-4,5-dimethyltetrazolium [3], 2,4,5-trimethyltetrazolium [4], and 1,5-diamino-4-H-tetrazolium [5]. Melting points for these cations combined with iodide, nitrate, and perchlorate anions range from  $-59\text{ }^{\circ}\text{C}$  to  $156\text{ }^{\circ}\text{C}$  and their liquid range can be up to  $229\text{ }^{\circ}\text{C}$ . A summary of energetic tetrazolium cations that have recently appeared in the literature and their melting points are given in Table 1 [3-6].

Synthesis of triazolium cations is easier than that of tetrazolium cations, hence, there have been many more studies of energetic triazolium than tetrazolium compounds. Triazolium cations have been successfully substituted with azido, diazido [4], and amino groups [3-6]. The successful synthesis of the triazolium cation is not so surprising due to its similarity to the popular imidazolium cation, but what is surprising is the use of the triazole ring as an ionic liquid anion. Ionic liquids typically contain a large asymmetric organic cation, which causes the ions to be poorly coordinated, but as shown by Katritzky et al., [7] the anion can be large as well. An ionic liquid, 1-butyl-3-methylimidazolium 3,5-dinitro-1,2,4-triazolate, containing a high energy planar anion, has been synthesized and has a low melting point of  $35\text{ }^{\circ}\text{C}$ . Delocalization of charge on the anion ring is caused by the nitro substituent groups, which also serve to increase the energy of the compound.

Interactions in ionic liquids are more complicated than those in simpler liquids, making them more difficult to understand on a molecular level. Theory can provide an excellent tool for understanding the structure and dynamics of ionic liquids. There have been several molecular dynamics simulations of ionic liquids, in order to model bulk properties, such as melting points, diffusion, and viscosity [8],[9]. Radial distribution

functions and densities have also been calculated [8],[10]. Predicted equilibrium structures of 1-alkyl-3-methylimidazolium ionic liquids with various anions and alkyl side chains have been found to compare well to experiment [11]. Dynamics simulations have revealed that 1-ethyl-3-methylimidazolium nitrate has diffusion properties similar to those of a supercooled liquid [12].

The solvent properties of ionic liquids and their propensity to be synthesized depend greatly on their acid-base properties, so the ability to predict these properties would be of great use. The more acidic the cation, the more difficult it will be to protonate the neutral ring to form an ionic liquid. Of the three neutral rings, imidazole, triazole, and tetrazole, the weakest base is tetrazole. Tetrazolium is therefore, the most difficult to synthesize. Acidity constants of triazole and tetrazole have been calculated using several semi-empirical methods [13].

In order to have low melting ionic liquids, the charge of at least one of the ions must be delocalized. MCSCF analysis of the triazolium cation shows that the electrons on the cation are shared between two resonance structures [2]. This study also investigated the effects of more energetic and less energetic substituent groups. For example, the nitrile group was proposed as a better substituent for high energy applications than an azide group. The structures of triazolium dinitramide systems were investigated using dimer pairs. A wide variety of geometries were found and the presence of small barriers for proton transfer from the cation to the anion show that deprotonation may be an important mechanism in decomposition of triazolium-based ionic liquids.

## Computational Methods

Initial structures were obtained by performing gas phase density functional theory (DFT) calculations on the isolated ions using the Becke three parameter Lee-Yang-Parr hybrid functional (B3LYP) [14, 15]. The basis sets used were 6-31G(d,p) [16-18], and 6-311G(d,p) [18, 19]. The DFT geometries and energies are compared to second order Moller-Plesset perturbation theory (MP2) calculations [20, 21]. A MCSCF population analysis [22] using Edmiston-Ruedenberg type localized molecular orbitals (LMO) [23] was carried out to investigate the amount of electron delocalization in the ring. The orbitals included in the MCSCF active space are both  $\pi$  orbitals, their corresponding antibonds, and the lone pair.

Calculations on ion pairs provide information about the fundamental interactions between the cation and the anion. The gas phase ion interactions can provide insight into the bulk liquid structure. Dimer pairs were optimized using DFT and MP2 methods and the 6-31+G(d)<sup>16</sup> [24, 25] basis set. Hessians (matrices of energy second derivatives) are used to determine if stationary points are minima or transition states. At the final MP2/6-311G(d,p) geometries, improved relative energies were obtained for some of the tetrazolium cation isomers, using singles and doubles coupled cluster theory with perturbative triples (CCSD(T)) [26, 27] with the 6-311G(d,p) and cc-pVTZ [28] basis sets.

Intrinsic reaction coordinate (IRC) calculations were used to connect transition states with reactants and products [29]. The step size used for the IRC calculations was 0.05 (amu)<sup>1/2</sup> bohr. All calculations were done with GAMESS [30, 31], and all molecules

were visualized with MacMolPlt [32].

## Results and Discussion

### Relative Energies of Tetrazolium Cations

The tetrazolium cation has four parent isomers (all R=H) labeled I, II, III, and IV (Figure 3). Each isomer has two possible resonance contributors. The relative energies of I, II, III, and IV are shown in Table 2. Isomer I is predicted by MP2 to be the lowest in energy, with isomer II only 1.9 kcal/mol higher in energy. The MP2 relative energy ordering is I<II<IV<III. In general, DFT and MP2 are in good agreement, although DFT slightly reverses the order of isomers I and II.

The relative energies of isomers I and II were also calculated using the CCSD(T) method at the MP2/6-311G(d,p) geometries. Using the 6-311G(d,p) and cc-pVTZ basis sets, isomer II is predicted to be lower in energy than I by 0.2 and 0.5 kcal/mol respectively. The open chain form of the cation, azido formidinium (V), shown in Figure 4, was also compared to the four parent isomers. At the MP2/6-311++G(d,p) geometry this isomer is 0.7 kcal/mol lower in energy than isomer I (Table 3). According to CCSD(T)/cc-pVTZ//MP2/6-31+G(d), isomer V is 1.8 kcal/mol higher in energy than isomer I, and 1.3 kcal/mol higher in energy than isomer II.

The large MP2/6-311G(d,p) barriers for proton transfer reactions between isomer I and isomers II, III, and IV (Figure 5) imply that movement of a proton on the ring is not likely.

Calculated MP2/6-311G(d,p)  $\sigma$  and  $\pi$  bond orders [33] (Figure 6) suggest that the

two double bonds in the ring are delocalized. The bond lengths between atoms in the rings do not exhibit any significant changes among the four parent isomers (Table 4). The bond lengths between atoms in the cation rings are consistent with a delocalized ring system (cf., 1.32 Å for a CN double bond and 1.34 Å for a NN double bond).

Bond lengths can suggest which resonance structures are favored for isomers I and III. (The two resonance structures for isomers II and IV are equivalent.) The nearly equal N1-N2 and N2-N3 bond lengths in isomer I (1.31 and 1.29 Å, respectively) suggest that resonance structures I and I' make similar contributions to the electronic structure of the ring, with perhaps a slight preference for I over I'. The two resonance structures for isomer III are likewise equally important as indicated by the equal N2-N3 and N3-N4 bond lengths and the nearly equal lengths of the N1-C5 and N4-C5 bonds.

MCSCF  $\pi$  LMO populations and  $\pi$  bond orders (Table 5) can provide a more sophisticated analysis of competing resonance structures [2]. The diagonal density matrix elements give the electron occupancy of the localized molecular orbitals. The off-diagonal elements give the bond orders. A positive bond order indicates a bonding interaction and a negative bond order indicates an antibonding interaction between the LMOs.

For isomer I, the  $\pi$  orbital populations on N1 and N3 are 1.42 and 1.37 respectively. In a resonance structure that was purely I, N1 would have a  $\pi$  population of 2.00 and all other atoms in the ring would have  $\pi$  populations of 1.00 (see Figure 3). If the structure was purely I', then N3 would have a  $\pi$  population of 2.00 and all other atoms in the ring would have  $\pi$  populations of 1.00 (cf., Figure 3). In reality both N1 and N3 have  $\pi$  populations of less than 1.5 electrons. This indicates that the ring is a hybrid



between I and I' and is delocalized. The difference in  $\pi$  orbital populations indicate that I is slightly favored over I'. In both I and I' C5-N4 is a double bond. This bond has a  $\pi$  bond order of 0.73, the largest of the five bonds. The N2-N3  $\pi$  bond order, a double bond in I, is 0.65. The N1-N2  $\pi$  bond order, is a double bond in I' is 0.57. Neither of these bond orders is close to 1.00 indicating once again that the ring is delocalized.

A similar analysis can be done for isomers II-IV showing that all the  $\pi$  electrons are delocalized on the cations. According to the  $\pi$  orbital populations in isomer III, the lone pair is distributed equally on N1 and N2. Similar comments apply to isomer II(IV), in which the lone pair is distributed equally on N1 and N4 (N2 and N3).

The relative energies of the parent isomers with a single substituent on a nitrogen or a carbon are shown in Table 6. The isomers with a substituent R' (on a nitrogen) are labeled I-A through IV-A (Figure 7a), the isomers with a substituent R'' (on the carbon) are labeled I-B through IV-B (Figure 7b), and the isomers with a substituent R''' (on a nitrogen) are labeled I-C through IV-C (Figure 7c). For all substituents, the relative energies remain the same as those of the parent isomers with no substitution.

A -NO<sub>2</sub> substituent does not bind well to a nitrogen of the tetrazolium ring: the NN distance is 2.4 Å, compared with a normal single NN bond distance of 1.430 Å as, for example, in N<sub>2</sub>H<sub>4</sub> [34]. Because of the lack of a strong NN bond, the nitro group easily changes positions on the ring. For example, III-A(NO<sub>2</sub>) converts to isomer I-A(NO<sub>2</sub>), with no barrier. A cation with a -NO<sub>2</sub> substituent bound to a ring nitrogen, is most likely an ion-dipole complex, in which the cation becomes a neutral tetrazole ring and the nitro group becomes an incipient cation. This is easily verified by examining the charge on the substituent -NO<sub>2</sub> group. The average of the Mulliken charges [35] on the

$-\text{NO}_2$  group for all isomers with  $-\text{NO}_2$  on N is +0.83. The average MP2/6-311G(d,p) binding energy of  $\text{NO}_2^+$  to a tetrazole ring is 22.8 kcal/mol.

A comparison of relative energies (averaged for all four parent isomers) for substitution on a C vs. N is shown in Table 7. Substitution at C is almost always energetically favored over substitution at N. The only exception is for the  $-\text{NO}_2$  substituent. The bond lengths within the ring do not change significantly from the parent isomer when a single substituent is present.

### Heats of Formation

The energy content of a heterocycle can be raised dramatically by increasing the number of nitrogen atoms in the ring. For example, the experimental heats of formation for imidazole, 1,2,4-triazole, and tetrazole are 14.0, 26.1, and 56.7 kcal/mol respectively [33].

In this work, heats of formation for the cation rings were calculated using isodesmic reactions and the Gaussian-2 (G2) method [36, 37], a multilevel method designed to obtain accurate thermochemistry. The G2 calculations were performed using Gaussian 94 [38]. Isodesmic reactions, in which the number of formal bond types is conserved, minimize the change in correlation energy [39], thereby reducing the error in a computed heat of formation.

The isodesmic reactions of each resonance structure are shown in Figure 8. For I and III each resonance structure has a different isodesmic reaction. The heats of formation for I and I' (III and III') are similar, and their average will be taken as a heat of formation for the composite I/I' (III/III') [2]. The largest difference in heats of formation

between resonance structures is 13.0 kcal/mol for the  $-\text{NO}_2$  substituent; the other differences are all less than 3 kcal/mol.

The heats of formation for the parent isomers are shown in column 2 of Table 8. These compare well to heats of formation that were calculated previously using Gaussian-3 [13]. The changes in heats of formation for substituted cations relative to the hydrogen substituted cations are shown in Table 9. For the most part, substitution destabilizes the ring, although, substitution by a fluorine or an amine on a carbon stabilizes the ring by up to 40 kcal/mol. However, an azide group or a nitrile group can increase the heat of formation of the ring by as much as 112 kcal/mol. Substitution with  $-\text{F}$ ,  $-\text{NH}_2$ , and  $-\text{NO}_2$  generally increases the heats of formation by about 20 kcal/mol.

### Proton Transfer Reactions

One possible reaction pathway for the simple ion pairs is proton transfer from the cation to a partner anion to form a neutral pair. The heats for the reaction  $\text{CN}_4\text{H}_3^+ + \text{Y}^- \rightarrow \text{CN}_4\text{H}_2 + \text{HY}$  (where  $\text{Y} = \text{NO}_3$ ,  $\text{ClO}_4$ , or  $\text{N}(\text{NO}_2)_2$ ) are shown in Table 10. All of the energy differences ( $\Delta E$ ) are exothermic, by 46-144 kcal/mol, and the  $\Delta E$ s for proton transfer to each of the three anions are similar. The heat of reaction for removal of  $\text{H}'''$ , shown in column three of Table 10, is more exothermic than the removal of  $\text{H}'$  (see Figure 3) because the 2,5-disubstituted neutral ring is 3.7 kcal/mol lower in energy than the 1,5-disubstituted neutral ring. The 1,3-disubstituted ring is considerably higher in energy. There are three possible positions for proton transfer to the dinitramide anion, but dinitramic acid is most stable with the proton on the center nitrogen, so this is the acid used when calculating the  $\Delta E$ s.

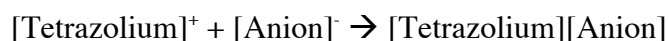
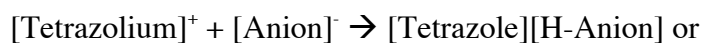
### Ion Pair Interactions

Ionic liquid dimer pairs were optimized with DFT and MP2 methods using the 6-31+G(d) basis set. ZPE corrections at the B3LYP/6-31+G(d) level of theory were used in all cases. The structures of the tetrazolium dimers with perchlorate and nitrate partners are shown in Figures 9 and 10, respectively. For the cation with perchlorate or nitrate, at both levels of theory a proton transfers from the cation to the anion during geometry optimization of the ion pair. Hydrogen bonding and other attractive electrostatic interactions are found to be important in the dimer structures. Optimizations give geometries in which the number of attractive electrostatic interactions is maximized. For pairs containing  $\text{HNO}_3$  or  $\text{HClO}_4$ , there is always one linear  $\text{O-H}\cdots\text{N}$  hydrogen bond. Hydrogen bond lengths vary from 1.795 Å to 1.846 Å for  $\text{HNO}_3$  and 1.771 Å to 1.822 Å for  $\text{HClO}_4$ . The majority of structures also contain a non-linear  $\text{N-H}\cdots\text{O}$  hydrogen bond or a  $\text{C-H}\cdots\text{O}$  attractive electrostatic interaction.

Tetrazolium dinitramide (Figure 11) pairs have a much wider variety of structures than tetrazolium nitrate or tetrazolium perchlorate pairs. This is because the dinitramide anion has the ability to bind a proton at three different positions (Figure 12). For  $\text{HN}(\text{NO}_2)_2$  pairs, hydrogen bond lengths vary from 1.721 Å to 1.942 Å. Once again hydrogen bonding and other electrostatic interactions are important for structures containing  $\text{HN}(\text{NO}_2)_2$ . However, six out of 19 structures do not contain a linear hydrogen bond at all. These structures usually contain weaker, nonlinear,  $\text{N-H}\cdots\text{N}$ ,  $\text{O-H}\cdots\text{N}$ , or  $\text{N-H}\cdots\text{O}$  attractive electrostatic interactions.

The relative energies of the pairs with  $\text{HNO}_3$  or  $\text{HClO}_4$  show that the lowest

energy pairs contain the 1,3-H substituted tetrazole isomer. For example, structure 1 in Figure 11 is 2.8 kcal/mol lower in energy than structure 6. This difference in energy can be attributed to the difference in energy of the 1,3-H substituted tetrazole ring (number 1) and the 1,2-H substituted tetrazole ring (number 6). The lowest energy structures with  $\text{HN}(\text{NO}_2)_2$ , contain the 1,3-H substituted tetrazole isomer and have the proton transferred to the central nitrogen of  $\text{N}(\text{NO}_2)_2^-$ . Also shown in Figures 9, 10, and 11 are the changes in energy for the reaction in which the infinitely separated anion and cation come together to form either an ion pair or a neutral pair by proton transfer from the cation to the anion:



For pairs in which a proton transfers, the neutral pair is lower in energy than the separated neutral products, due to the stabilization from electrostatic interactions in the neutral dimer products. The average dimer stabilization is 7.3, 9.6, and 8.4 kcal/mol for  $[\text{HNO}_3]$ ,  $[\text{HClO}_4^-]$ , and  $[\text{HN}(\text{NO}_2)_2]$  respectively.

At the DFT level of theory there are some stable  $\text{HN}(\text{NO}_2)_2^-$ -cation pair geometries; however when those DFT geometries are optimized with MP2, the acidic proton usually transfers to the anion. Only one stable anion-cation pair was found at the MP2 level of theory. This ion pair is structure 13 in figure 11. The ion pair is higher in energy by 18.9 kcal/mol than the lowest energy neutral pair at MP2/6-31+G(d). In this structure the N-H bond length is stretched to 1.076 Å as compared to 1.019 Å for the non-acidic hydrogen. The hydrogen bond length is also much shorter at 1.598 Å. The

length of the hydrogen bonds show that the hydrogen bond in the ionic structure is much stronger than the hydrogen bond in the various neutral structures. The MP2 barrier for proton transfer from the cation to the anion of structure 13 of Figure 11 is 0.4 kcal/mol (Figure 13), however when ZPE corrections are accounted for, the barrier disappears. For all dimer pairs, proton transfer from a cation to the nitrogen of the dinitramide anion is favored energetically over proton transfer to one of the oxygens of the dinitramide anion.

Gas phase calculations on an ionic pair can, of course, only give an approximation to the true interactions in a crystalized ionic liquid. Proton transfer from the cation to the anion should be less likely in the crystal or in bulk liquid. For example, in studies of ammonium salts, proton transfer occurs in the isolated gas phase ion pair, but stable ion pairs are found when two anions and two cations are present [40]. MP2/6-31++G(d,p) calculations on 1,2,4-triazolium dinitramide typically do not give stable ion pairs [2]. The most recent MP2 calculations done on three ion pairs of 1,2,4-triazolium dinitramide, show that the 6 ion cluster is only 1.0 kcal/mol higher in energy than the 6 neutral cluster [41]. Whether the ionic form or the neutral form is lower in energy for two ion pairs is still under investigation. Future studies on larger clusters of ionic pairs are needed to more fully understand the interactions in the bulk liquid.

## Conclusion

In this work, tetrazolium cations I and II were established to be the lowest energy isomers, for the parent isomers as well as for all substituted isomers. The DFT and MP2 energies are generally in good agreement. The relative energy of the open chain form of

the cation is predicted to be only slightly higher in energy than isomers I and II. A MCSCF  $\pi$  orbital analysis indicates that the electrons in the cation ring are delocalized. Calculated heats of formation show that the tetrazolium cation ring has the potential to release large amounts of energy during decomposition and thus has excellent potential as a high energy fuel. This is especially true when the ring is substituted with  $-\text{N}_3$  or  $-\text{CN}$ . When a cation is paired with oxygen rich anions, a single gas phase ion pair was not generally found to be stable. A proton transfers without barrier from the cation to the anion to form a neutral pair.

### **Acknowledgements**

This work was supported by a grant from the Air Force Office of Scientific Research. The authors are grateful to Drs. Michael Schmidt and Greg Drake for many helpful discussions.

- (1) Rogers, R. D.; Seddon, K. R., Eds. *Ionic Liquids; Industrial Applications to Green Chemistry*: Washington DC, 2002.
- (2) Schmidt, M. W.; Gordon, M. S.; Boatz, J. A. *J. Phys. Chem. A* **2005**, *109*, 7285-7295.
- (3) Xue, H.; Arritt, S. W.; Twamley, B.; Shreeve, J. n. M. *Inorganic Chemistry* **2004**, *43*, 7972-7977.
- (4) Xue, H.; Gao, Y.; Twamley, B.; Shreeve, J. n. M. *Chemistry of Materials* **2005**, *17*, 191-198.
- (5) Drake, G. W.; Hawkins, T. W.; Boatz, J.; Hall, L.; Vij, A. *Propellants Explosives and Pyrotechnics* **2005**, *30*, 156-163.
- (6) Drake, G.; Hawkins, T.; Brand, A.; Hall, L.; McKay, M. *Propellants, Explosives, Pyrotechnics* **2003**, *28*, 174-180.
- (7) Katritzky, A. R.; Singh, S.; Kirichenko, K.; Holbrey, J. D.; Smiglak, M.; Reichert, W. M.; Rogers, R. D. *Chemical Communications (Advance Article)* **2005**.
- (8) Velardez, G. F.; Alavi, S.; Thompson, D. L. *The Journal of Chemical Physics* **2003**, *119*, 6698-6708.
- (9) Yan, T.; Burnham, C. J.; Popolo, M. G. D.; Voth, G. A. *The Journal of Physical Chemistry B* **2004**, *108*, 11877-11879.
- (10) Margulis, C. J.; Stern, H. A.; Berne, B. J. *Journal of Physical Chemistry B* **2002**, *106*, 46.
- (11) Urahata, S. M.; Ribeiro, M. C. C. *The Journal of Chemical Physics* **2004**, *120*, 1855-1863.
- (12) Del Popolo, M. G.; Voth, G. A. *Journal of Physical Chemistry B* **2004**, *108*, 1744-1752.
- (13) Satchell, J. F.; Smith, B. J. *Physical Chemistry Chemical Physics* **2002**, *4*, 4314-4318.
- (14) Vosko, S. J.; Wilk, L.; Nusair, M. *The Canadian Journal of Physics* **1980**, *58*, 1200-1211.
- (15) Becke, A. D. *Journal of Chemical Physics* **1993**, *98*, 5648-5652.
- (16) Ditchfield R.; Hehre W. J.; Pople J. A. *The Journal of Chemical Physics* **1971**, *54*, 724.
- (17) Hehre WJ; Ditchfield R; Pople J. A. *The Journal of Chemical Physics* **1972**, *56*, 2257.
- (18) Hariharan P. C., Pople J. A. *Theoretical Chemistry Accounts: Theory, Computation, and Modeling (Theoretica Chimica Acta) (Historical Archive)* **1973**, *28*, 213.
- (19) Krishnan, R.; Binkley, J. S.; Seeger, R.; Pople, J. A. *The Journal of Chemical Physics* **1980**, *72*, 650-654.
- (20) Møller, C.; Plesset, M. S. *Physical Review* **1934**, *46*, 618-622.
- (21) Fletcher, G. D.; Rendell, A. P.; Sherwood, P. *Molecular Physics* **1997**, *91*, 431-438.
- (22) Schmidt, M. W.; Gordon, M. S. *Annu. Rev. Phys. Chem.* **1998**, *49*, 233-266.
- (23) Edmiston, C.; Ruedenberg, K. *Rev. Mod. Phys.* **1963**, *35*.
- (24) Gordon M. S. *Chemical Physics Letters* **1980**, *76*, 163
- (25) Clark T.; Chandrasekhar J.; Spitznagel G. W.; Schleyer PvR *Journal of Computational Chemistry* **1983**, *4*, 294



- (26) Raghavachari, K.; Trucks, G. W.; Pople, J. A.; Headgordon, M. *Chemical Physics Letters* **1989**, *157*, 479-483.
- (27) Piecuch, P.; Kucharski, S. A.; Kowalski, K.; Musial, M. *Computer Physics Communications* **2000**, *149*, 71-96.
- (28) Dunning Jr., T. H. *The Journal of Chemical Physics* **1989**, *90*, 1007-1023.
- (29) Garrett, B. C.; Redmon, M. J.; Steckler, R.; Truhlar, D. G.; Baldrige, K. K.; Bartol, D.; Schmidt, M. W.; Gordon, M. S. *Journal of Physical Chemistry* **1988**, *92*, 1476-1488.
- (30) Schmidt, M. W.; Baldrige, K. K.; Boatz, J. A.; Elbert, S. T.; Gordon, M. S.; Jensen, J. H.; Koseki, S.; Matsunaga, N.; Nguyen, K. A.; Su, S. J.; Windus, T. L.; Dupuis, M.; Montgomery, J. A. *Journal of Computational Chemistry* **1993**, *14*, 1347-1363.
- (31) Schmidt, M. W.; Gordon, M. S. In *Theory and Applications of Computational Chemistry: The First Forty Years*; Dykstra, C. E., Frenking, G., Kim, K. S., Scuseria, G. E., Eds.; Elsevier, 2005.
- (32) Bode, B. M.; Gordon, M. S. *Journal of Molecular Graphics & Modelling* **1999**, *16*, 133-138.
- (33) Mayer, I. *Chem. Phys. Lett.* **1983**, *97*, 270-274.
- (34) DeFrees, D. J.; Raghavachari, K.; Schlegel, H. B.; Pople, J. A. *J. Am. chem. Soc.* **1982**, *104*, 5576-5580.
- (35) Mulliken, R. S. *J. Chem. Phys* **1955**, *23*, 1833-1840, 1841-1846, 2338-2342, 2343-2346.
- (36) Curtiss, L. A.; Raghavachari, K.; Redfern, P. C.; Pople, J. A. *Journal of Chemical Physics* **1997**, *106*, 1063-1079.
- (37) Curtiss, L. A.; Raghavachari, K.; Trucks, G. W.; Pople, J. A. *Journal of Chemical Physics* **1991**, *94*, 7221-7230.
- (38) Frisch, M. J.; G. W. Trucks; H. B. Schlegel; P. M. W. Gill; B. G. Johnson; M. A. Robb; J. R. Cheeseman; T. Keith; G. A. Petersson; J. A. Montgomery; K. Raghavachari; M. A. Al-Laham; V. G. Zakrzewski; J. V. Ortiz; J. B. Foresman; J. Cioslowski; B. B. Stefanov; A. Nanayakkara; M. Challacombe; C. Y. Peng; P. Y. Ayala; W. Chen; M. W. Wong; J. L. Andres; E. S. Replogle; R. Gomperts; R. L. Martin; D. J. Fox; J. S. Binkley; D. J. Defrees; J. Baker; J. P. Stewart; M. Head-Gordon; Gonzalez, C.; Pople, J. A. *Gaussian, Inc., Pittsburgh PA* **1995**.
- (39) Hehre, W. J.; Ditchfield, R.; Radom, L.; Pople, J. A. *J. Am. chem. Soc.* **1970**, *92*, 4796-4801.
- (40) Alavi, S.; Thompson, D. L. *The Journal of Chemical Physics* **2003**, *119*, 4274.
- (41) Li, H.; Gordon, M. S. **2005**, *in preparation*.

**Table 1: Energetic tetrazolium cations, their melting points ( $T_m$ ), thermal decomposition temperatures ( $T_d$ ), and glass transition temperature ( $T_g$ ).**

1-Amino-4,5-dimethyltetrazolium Iodide <sup>a</sup>	$T_m$ 121 °C	
1-Amino-4,5-dimethyltetrazolium Nitrate <sup>a</sup>	$T_g$ -59 °C	$T_d$ 170 °C
1-Amino-4,5-dimethyltetrazolium Perchlorate <sup>a</sup>	$T_m$ 51 °C	$T_d$ 182 °C
2-Amino-4,5-dimethyltetrazolium Iodide <sup>a</sup>	$T_m$ 124 °C	
2-Amino-4,5-dimethyltetrazolium Nitrate <sup>a</sup>	$T_m$ 94 °C	$T_d$ 173 °C
2-Amino-4,5-dimethyltetrazolium Perchlorate <sup>a</sup>	$T_m$ 140 °C	$T_d$ 238 °C
2,4,5-Trimethyltetrazolium Iodide <sup>b</sup>	$T_m$ 156 °C	
2,4,5-Trimethyltetrazolium Nitrate <sup>b</sup>	$T_m$ 94 °C	$T_d$ 193 °C
2,4,5-Trimethyltetrazolium Perchlorate <sup>b</sup>	$T_m$ 133 °C	$T_d$ 315 °C
1,5-Diamino-4-H-Tetrazolium Perchlorate <sup>c</sup>	$T_m$ 125-130 °C	

<sup>a</sup> from Xue, Twamley, and Schreeve<sup>3</sup>, <sup>b</sup> from Xue, Gao, Twamley, and Schreeve<sup>4</sup>, <sup>c</sup> from Drake, Hawkins, Boatz, Hall, Vij<sup>5</sup>

**Table 2: Relative energies (kcal/mol) of Isomers I, II, III, and IV.**

Cation	B3LYP/6-31G(d,p)	B3LYP/6-311G(d,p)	MP2/6-31G(d,p)	MP2/6-311G(d,p)
I	0	0	0	0
II	-0.6	-0.4	1.4	1.9
III	16	16.2	19.1	19.2
IV	14.9	14.7	15.2	14.7

**Table 3: Relative energies (kcal/mol) of the closed chain isomers I, II, and the open chain isomer, V, using CCSD(T).**

	MP2/6-311++G(d,p)	CCSD(T)/cc-PVTZ// MP2/6-311++G(d,p)	CCSD(T)/6-311G(d,p)// MP2/6-311++G(d,p)
I	0.0	0.0	0.0
II	1.9	-0.5	-0.2
V	-0.7	1.8	1.6

**Table 4: Bond lengths (Angstroms) in the ring for isomers I through IV.**

	C5-N1	N1-N2	N2-N3	N3-N4	N4-C5
I	1.36	1.31	1.29	1.33	1.31
II	1.33	1.35	1.30	1.35	1.33
III	1.35	1.32	1.32	1.32	1.34
IV	1.35	1.31	1.32	1.31	1.35

**Table 5: MCSCF  $\pi$  orbital populations and bond orders.**

	$\pi$ orbital populations					Total bonding
	N1	N2	N3	N4	C5	
I	1.42	1.10	1.37	1.12	0.98	1.93
II	1.44	1.09	1.09	1.44	0.94	1.92
III	1.46	1.46	1.04	1.10	0.95	1.91
IV	1.07	1.43	1.43	1.07	0.99	1.94

	Adjacent $\pi$ bond orders				
	C5-N1	N1-N2	N2-N3	N3-N4	N4-N5
I	0.55	0.57	0.65	0.48	0.73
II	0.65	0.44	0.77	0.44	0.65
III	0.61	0.44	0.60	0.62	0.64
IV	0.64	0.56	0.50	0.56	0.64

	Next neighbor $\pi$ bond orders (antibonding)				
	C5-N2	N1-N3	N2-N4	N3-C5	N4-N1
I	-0.22	-0.30	-0.27	-0.11	-0.15
II	-0.18	-0.19	-0.19	-0.18	-0.29
III	-0.30	-0.33	-0.22		-0.15
IV	-0.14	-0.34	-0.34	-0.14	

**Table 6: MP2/6-311G(d,p) relative energies (kcal/mol) isomers with a single substitution on a nitrogen or a carbon. (See Figure 7 for notation.)**

R' =	I-A	II-A	III-A	IV-A
H	0.0	1.9	19.1	14.7
F	0.0	3.4	18.3	12.6
CN	0.0	2.6	18.6	14.4
N <sub>3</sub>	0.0	5.3	16.8	16.0
NH <sub>2</sub>	0.0	1.8	17.1	13.0
NO <sub>2</sub>	0.0	2.7		4.9

R'' =	I-B	II-B	III-B	IV-B
H	0.0	1.9	19.1	14.7
F	0.0	5.0	22.6	16.8
CN	0.0	1.3	19.2	14.6
N <sub>3</sub>	0.0	2.9	15.4	11.0
NH <sub>2</sub>	0.0	3.5	16.3	11.7
NO <sub>2</sub>	0.0	2.5	17.8	15.6

R''' =	I-C	II-C	III-C	IV-C
H	0.0	1.9	19.1	14.7
F	0.0	2.3	22.1	14.0
CN	0.0	1.5	19.9	14.9
N <sub>3</sub>	0.0	1.6	20.1	9.6
NH <sub>2</sub>	0.0	1.0	18.2	9.4
NO <sub>2</sub>	0.0	1.1	13.5	3.3

**Table 7: MP2/6-311G(d,p) average energy differences between substitution at N and C on the tetrazolium ring.**

Average Values ( $E_C - E_N$ ):	
F	-56.9 kcal/mol
CN	-20.1 kcal/mol
N <sub>3</sub>	-30.0 kcal/mol
NH <sub>2</sub>	-27.9 kcal/mol
NO <sub>2</sub>	+6.0 kcal/mol

**Table 8: Heats of formation (kcal/mol), from G2 theory, for parent isomers.**

	Calculated G3 Heats of Formation <sup>a</sup>	Calculated G2 Heats of Formation <sup>b</sup>
I	248.0	245.1
II	247.1	246.9
III	263.7	264.3
IV	262.8	259.8

<sup>a</sup> G3 Heats of Formation are taken from Satchell and Smith<sup>13</sup>. <sup>b</sup> From this work.

**Table 9: Changes in heats of formation (kcal/mol), from G2 theory, due to substituents, relative to parent compounds. Refer to Figure 3 for structures.**

R'=	I	I'	average	R''=	I = I'	R'''=	I	I'	average
H	0.0	0.0	0.0	H	0.0	H	0.0	0.0	0.0
F	17.1	17.8	17.5	F	-37.5	F	19.9	20.6	20.2
CN	70.7	71.7	71.2	CN	51.0	CN	70.5	71.5	71.0
N <sub>3</sub>	108.6	111.4	110.0	N <sub>3</sub>	79.7	N <sub>3</sub>	109.9	112.8	111.3
NH <sub>2</sub>	18.2	18.9	18.6	NH <sub>2</sub>	-10.0	NH <sub>2</sub>	20.7	21.4	21.0
NO <sub>2</sub>	31.1	18.1	24.6	NO <sub>2</sub>	18.0	NO <sub>2</sub>	32.8	19.7	26.3

R'=	II	II'	average	R''=	II = II'	R'''=	II	II'	average
H	0.0	0.0	0.0	H	0.0	H	0.0	0.0	0.0
F	20.3	21.0	20.6	F	-36.0	F	20.3	21.0	20.7
CN	70.2	71.2	70.7	CN	51.7	CN	70.1	71.1	70.6
N <sub>3</sub>	109.6	112.5	111.0	N <sub>3</sub>	83.1	N <sub>3</sub>	109.6	112.5	111.1
NH <sub>2</sub>	19.9	20.6	20.3	NH <sub>2</sub>	-10.0	NH <sub>2</sub>	19.8	20.5	20.1
NO <sub>2</sub>	32.0	18.9	25.4	NO <sub>2</sub>	18.6	NO <sub>2</sub>	32.0	18.9	25.4

R'=	III	III'	average	R''=	III = III'	R'''=	III	III'	average
H	0.0	0.0	0.0	H	0.0	H	0.0	0.0	0.0
F	20.5	21.2	20.8	F	-38.4	F	22.8	23.5	23.1
CN	70.8	71.8	71.3	CN	50.3	CN	71.2	72.3	71.8
N <sub>3</sub>	104.8	107.6	106.2	N <sub>3</sub>	77.3	N <sub>3</sub>	110.8	113.7	112.2
NH <sub>2</sub>	15.4	16.0	15.7	NH <sub>2</sub>	-12.1	NH <sub>2</sub>	19.8	20.4	20.1
NO <sub>2</sub>				NO <sub>2</sub>	16.6	NO <sub>2</sub>	27.1	14.0	20.6

R'=	IV	IV'	average	R''=	IV = IV'	R'''=	IV	IV'	average
H	0.0	0.0	0.0	H	0.0	H	0.0	0.0	0.0
F	19.2	19.9	19.5	F	-39.6	F	19.2	19.9	19.6
CN	70.7	71.7	71.2	CN	50.7	CN	70.7	71.7	71.2
N <sub>3</sub>	104.9	107.8	106.3	N <sub>3</sub>	81.0	N <sub>3</sub>	104.8	107.7	106.3
NH <sub>2</sub>	15.3	15.9	15.6	NH <sub>2</sub>	-11.7	NH <sub>2</sub>	15.4	16.1	15.7
NO <sub>2</sub>	21.3	8.3	14.8	NO <sub>2</sub>	18.9	NO <sub>2</sub>	21.4	8.3	14.9

**Table 10: Heats of proton transfer reaction (kcal/mol) for anion =  $\text{NO}_3^-$ ,  $\text{ClO}_4^-$ , and  $\text{N}(\text{NO}_2)_2^-$  for deprotonation at  $\text{H}'$ ,  $\text{H}''$ , &  $\text{H}'''$ . (See Figure 3)**

Cation	anion	$\text{H}'$	$\text{H}''$	$\text{H}'''$
I	$\text{NO}_3^-$	-124.8	-86.1	-128.5
	$\text{ClO}_4^-$	-102.6	-63.9	-106.3
	$\text{N}(\text{NO}_2)_2^-$	-112.0	-73.3	-115.7
II	$\text{NO}_3^-$	-126.6	-103.7	same as $\text{H}'$
	$\text{ClO}_4^-$	-104.4	-81.5	
	$\text{N}(\text{NO}_2)_2^-$	-113.9	-90.9	
III	$\text{NO}_3^-$	-143.7	-85.9	-147.4
	$\text{ClO}_4^-$	-121.5	-63.7	-125.3
	$\text{N}(\text{NO}_2)_2^-$	-131.0	-73.1	-134.7
IV	$\text{NO}_3^-$	same as $\text{H}'$	-68.9	-142.9
	$\text{ClO}_4^-$		-46.7	-120.8
	$\text{N}(\text{NO}_2)_2^-$		-56.2	-130.2

Figure 1: Imidazolium (a), triazolium (b), and tetrazolium (c) cations.

Figure 2: Nitrate, perchlorate and dinitramide anions (Oxygen=red, nitrogen=blue, chlorine=green).

Figure 3: Resonance structures of isomers I-IV.

Figure 4: The open chain isomer, azido formidinium, V.

Figure 5: MP2/6-311G(d,p) IRC for proton transfer between isomer I and isomers II, III, and IV, kcal/mol.

Figure 6: Isomers I-IV with calculated bond orders in red.

Figure 7: Isomers with a single substitution on a nitrogen or a carbon.

Figure 8: Isodesmic reactions for all resonance structures.

Figure 9: Optimized structures (Å) and MP2 and B3LYP (in parentheses) relative energies (kcal/mol) for proton transferred structures that result from optimization of initial geometries of a tetrazolium cation paired with a  $\text{NO}_3^-$  anion. MP2 heats of reaction (in brackets) in kcal/mol for the reaction: Tetrazolium +  $\text{NO}_3^- \rightarrow [\text{Tetrazole}][\text{H-NO}_3]$ .

Figure 10: Optimized structures (Å) and MP2 and B3LYP (in parentheses) relative energies (kcal/mol) for proton transferred structures that result from optimization of initial geometries of a tetrazolium cation paired with a  $\text{ClO}_4^-$  anion. MP2 heats of reaction (in brackets) in kcal/mol for the reaction: Tetrazolium +  $\text{ClO}_4^- \rightarrow [\text{Tetrazole}][\text{H-ClO}_4]$ .

Figure 11: Optimized structures (Å) and MP2 and B3LYP (in parentheses) relative energies (kcal/mol) of the tetrazolium cation paired with a  $\text{N}(\text{NO}_2)_2^-$  anion. MP2 heats of reaction (in brackets) in kcal/mol for the reaction: Tetrazolium +  $\text{N}(\text{NO}_2)_2^- \rightarrow [\text{Tetrazole}][\text{HN}(\text{NO}_2)_2]$  or (see text)  $[\text{Tetrazolium}][\text{N}(\text{NO}_2)_2]$ .

Figure 12: Three different geometries of dinitramic acid.

Figure 13: The MP2/6-31+G(d) potential energy surface for proton transfer from the 1,4,5-tetrazolium cation to the dinitramide anion to form 1,5-tetrazole and dinitramic acid. The relative energies including ZPE corrections are in parenthesis. Relative energies in kcal/mol.



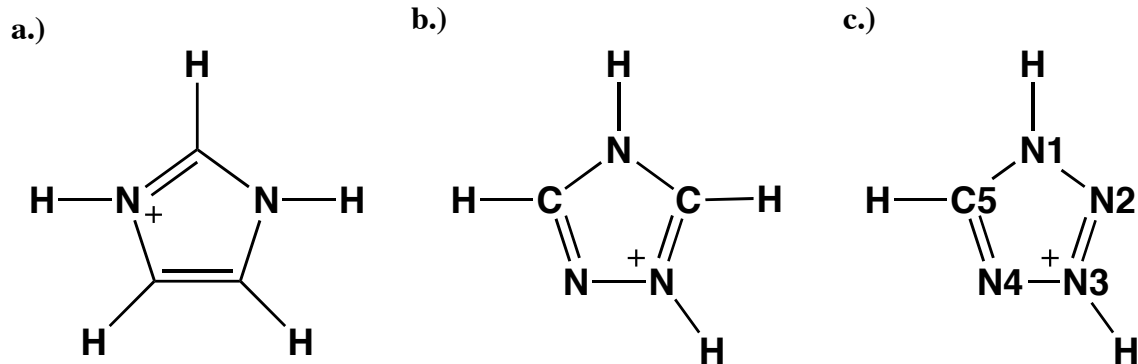


Figure 1: Imidazolium (a), 1,2,4-triazolium (b), and tetrazolium (c) cations.

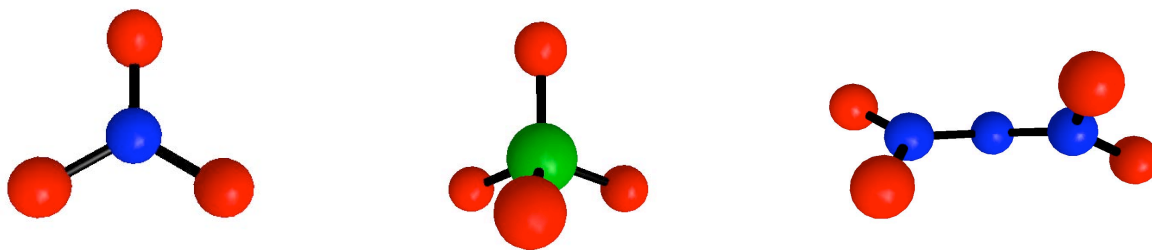


Figure 2: Nitrate, perchlorate and dinitramide anions (Oxygen=red, nitrogen=blue, chlorine=green).

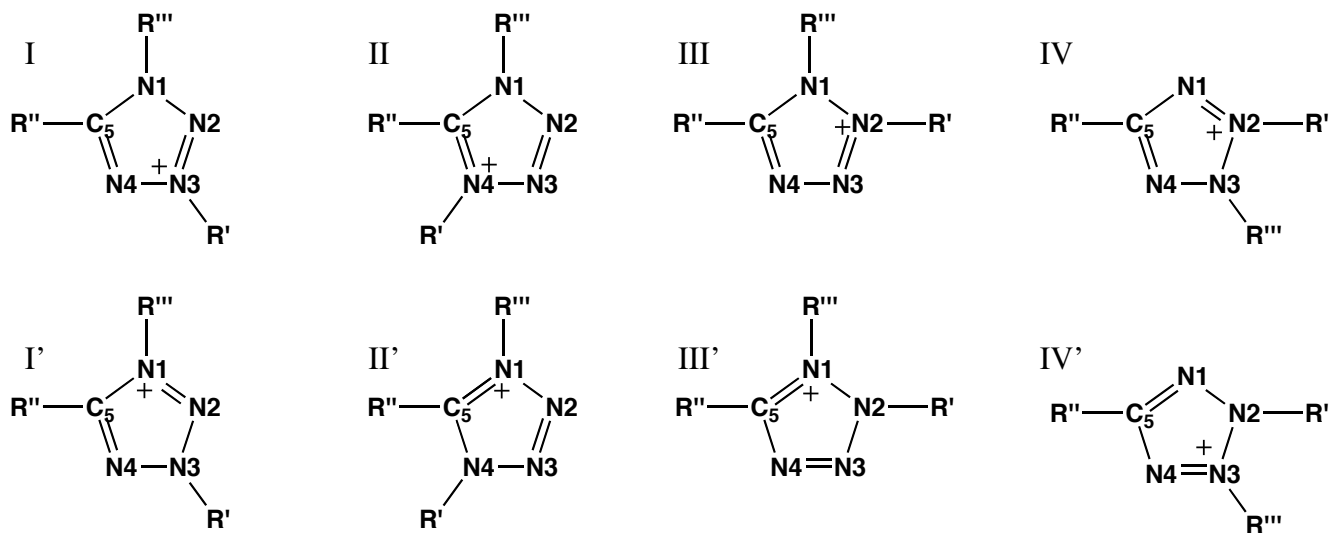


Figure 3: Resonance structures of isomers I-IV.

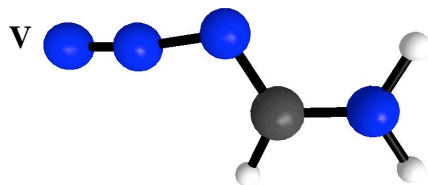


Figure 4: The open chain isomer, azido formidinium, V.

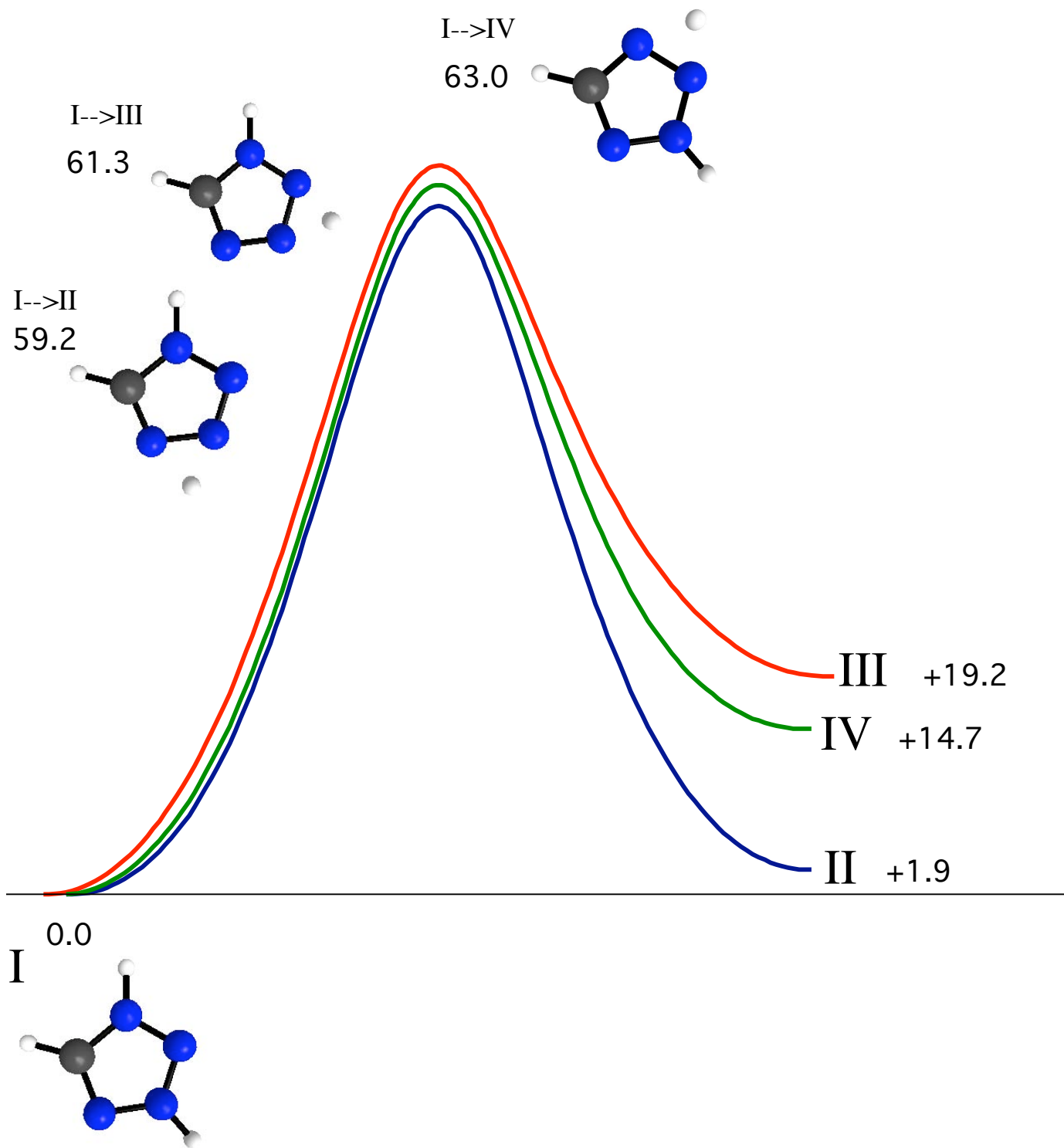


Figure 5: MP2/6-311G(d,p) IRC for proton transfer between isomer I and isomers II, III, and IV, kcal/mol.

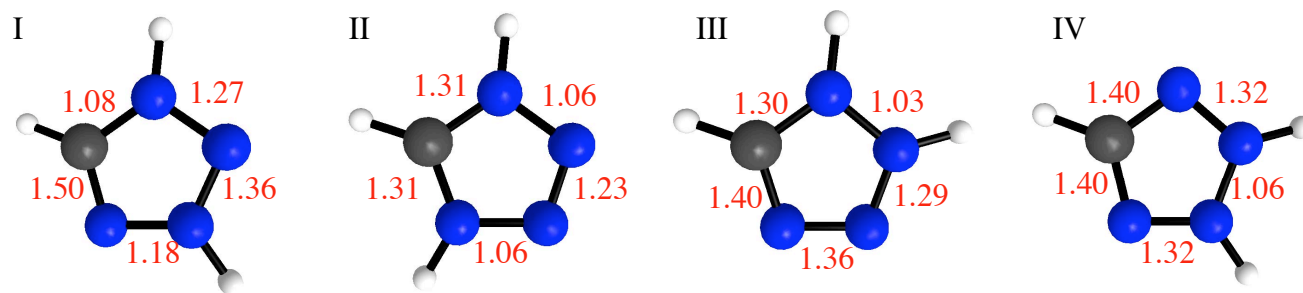
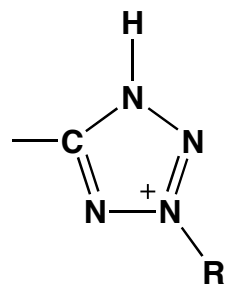


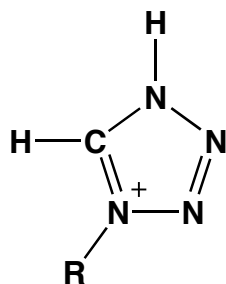
Figure 6: Isomers I-IV with calculated MP2 bond orders in red.

)

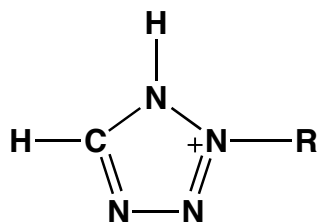
-A



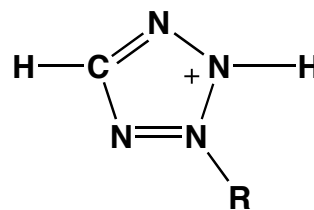
II-A



III-A

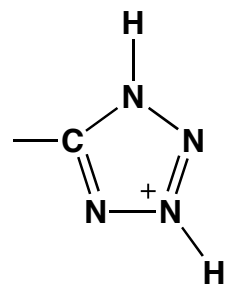


IV-A

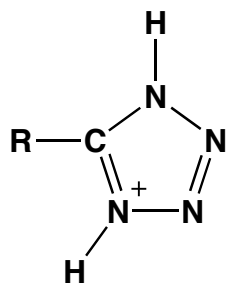


)

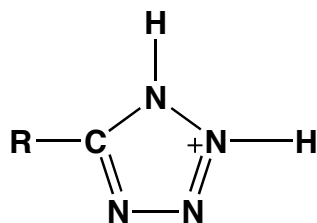
I-B



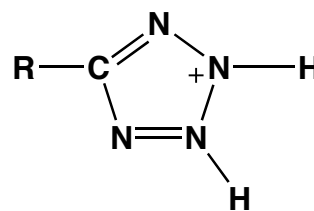
II-B



III-B

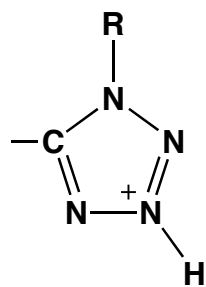


IV-B

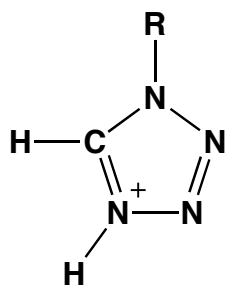


)

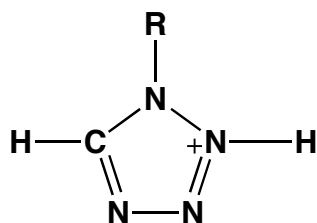
C



II-C



III-C



IV-C

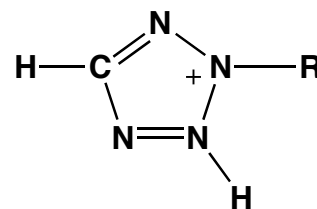


Figure 7: Isomers with a single substitution on a nitrogen or a carbon.

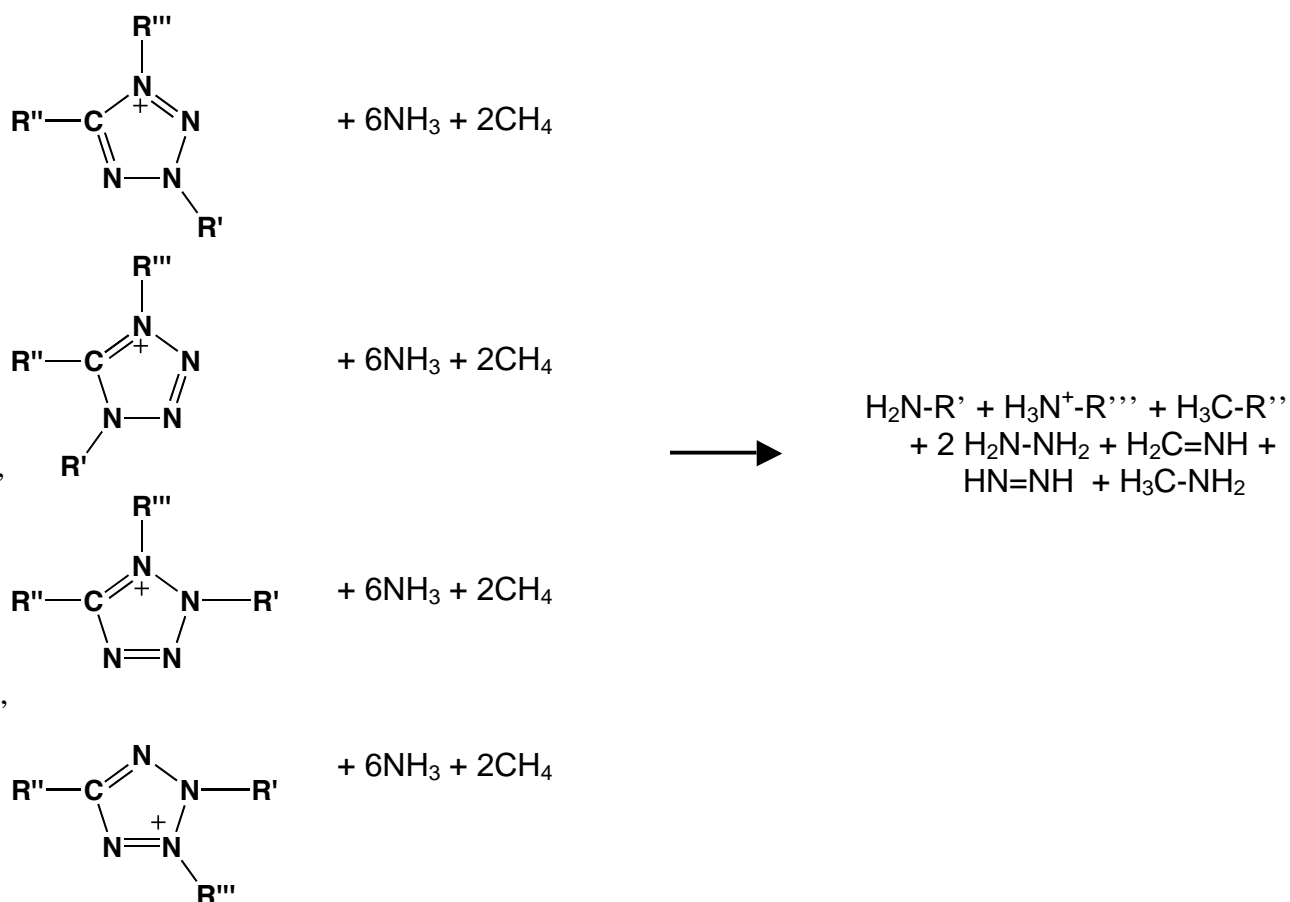
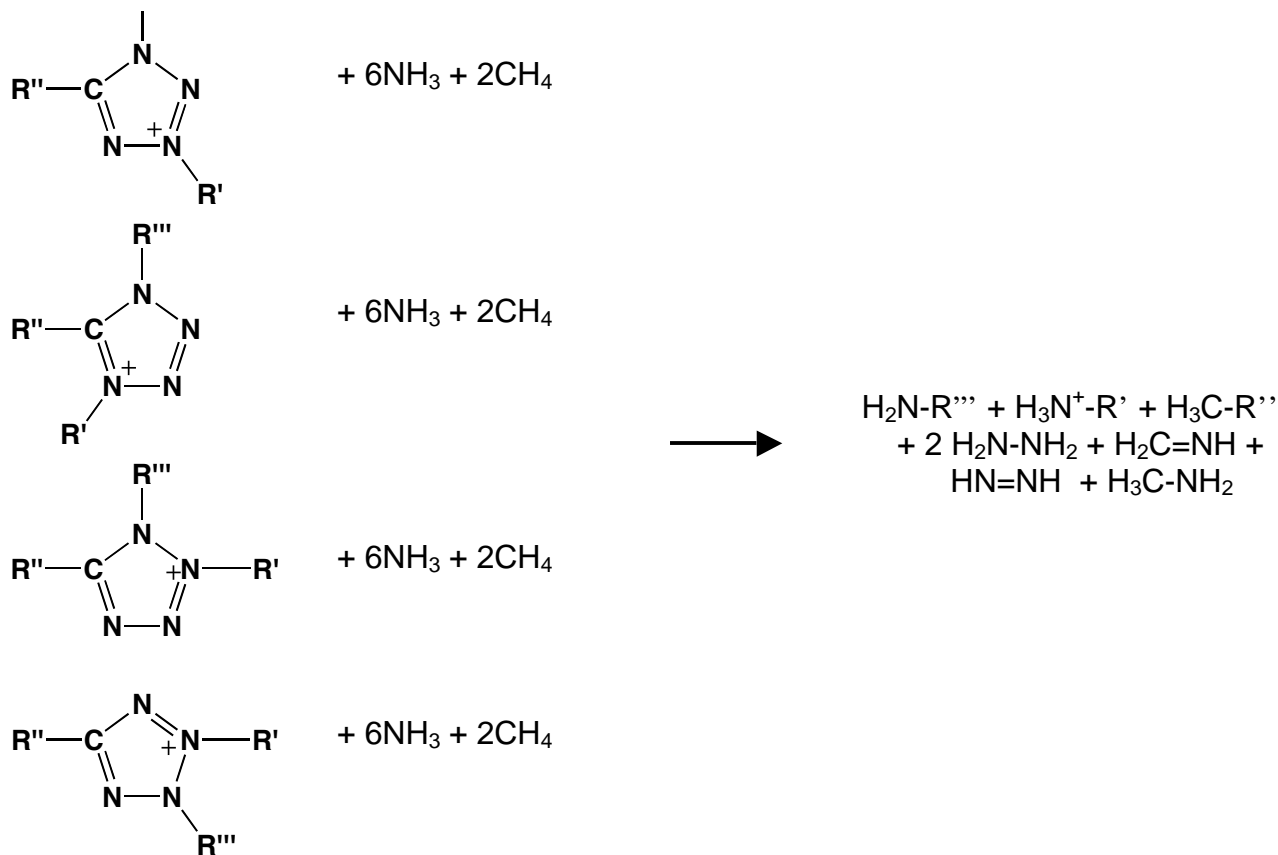


Figure 8: Isodesmic reactions for all resonance structures.

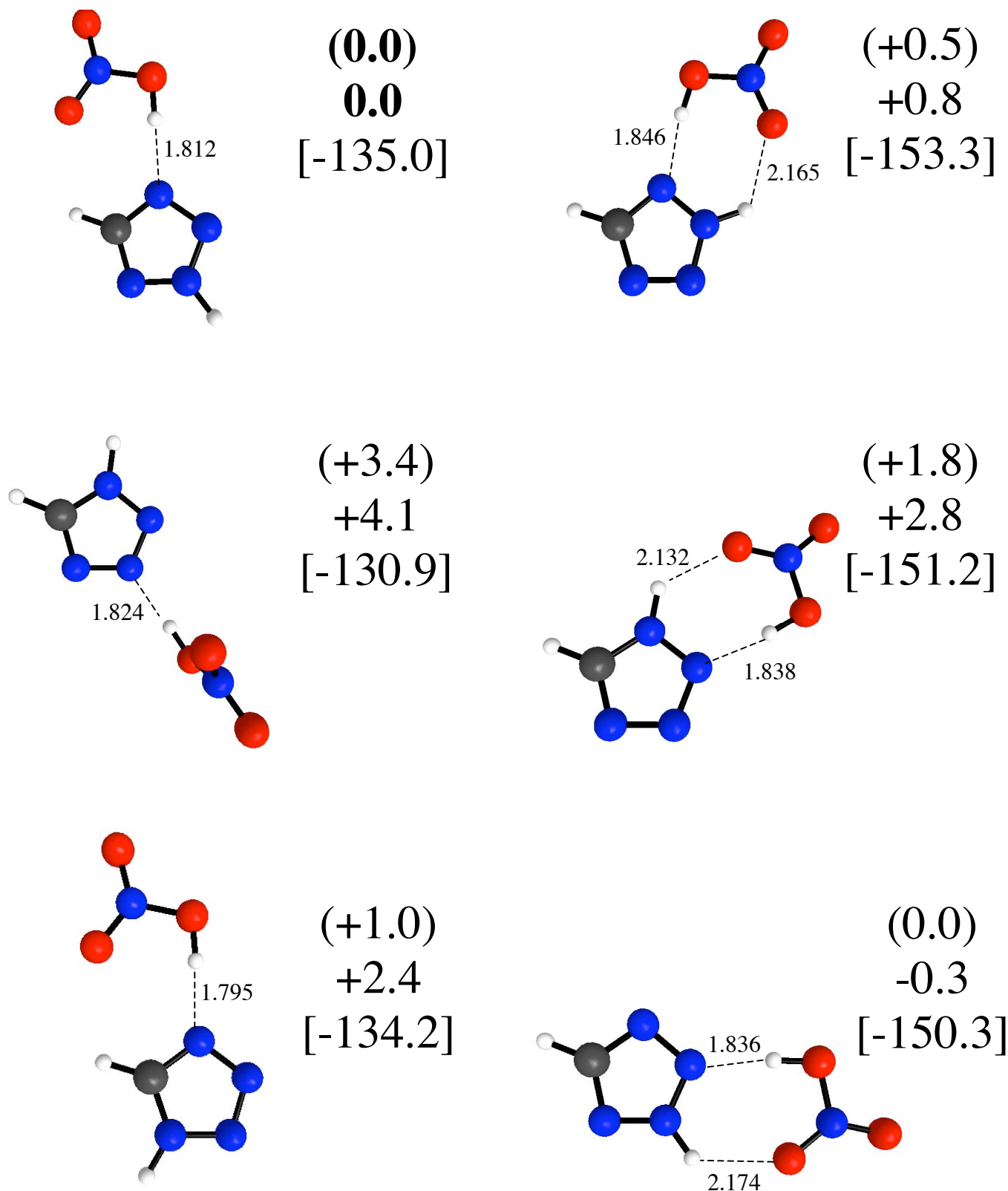


Figure 9: Optimized structures (Å) and MP2 and B3LYP (in parentheses) relative energies (kcal/mol) for proton transferred structures that result from optimization of initial geometries of a tetrazolium cation paired with a  $\text{NO}_3^-$  anion. MP2 heats of reaction (in brackets) in kcal/mol for the reaction:  $\text{Tetrazolium} + \text{NO}_3^- \rightarrow [\text{Tetrazole}][\text{H-NO}_3]$ .

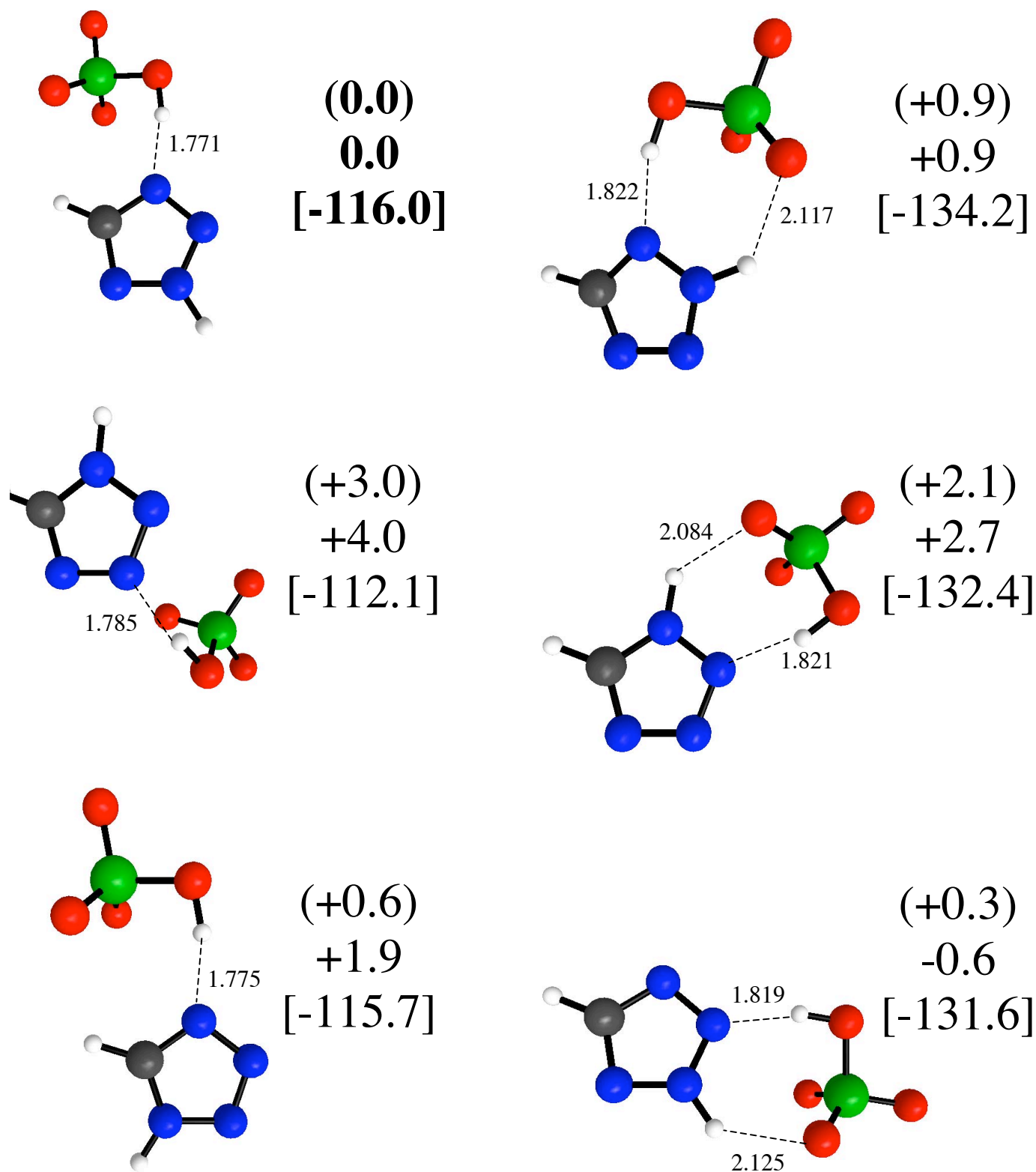


Figure 10: Optimized structures (Å) and MP2 and B3LYP (in parentheses) relative energies (kcal/mol) for proton transferred structures that result from optimization of initial geometries of a tetrazolium cation paired with a  $\text{ClO}_4^-$  anion. MP2 heats of reaction (in brackets) in kcal/mol for the reaction:  $\text{Tetrazolium} + \text{ClO}_4^- \rightarrow [\text{Tetrazole}][\text{H-ClO}_4]$ .



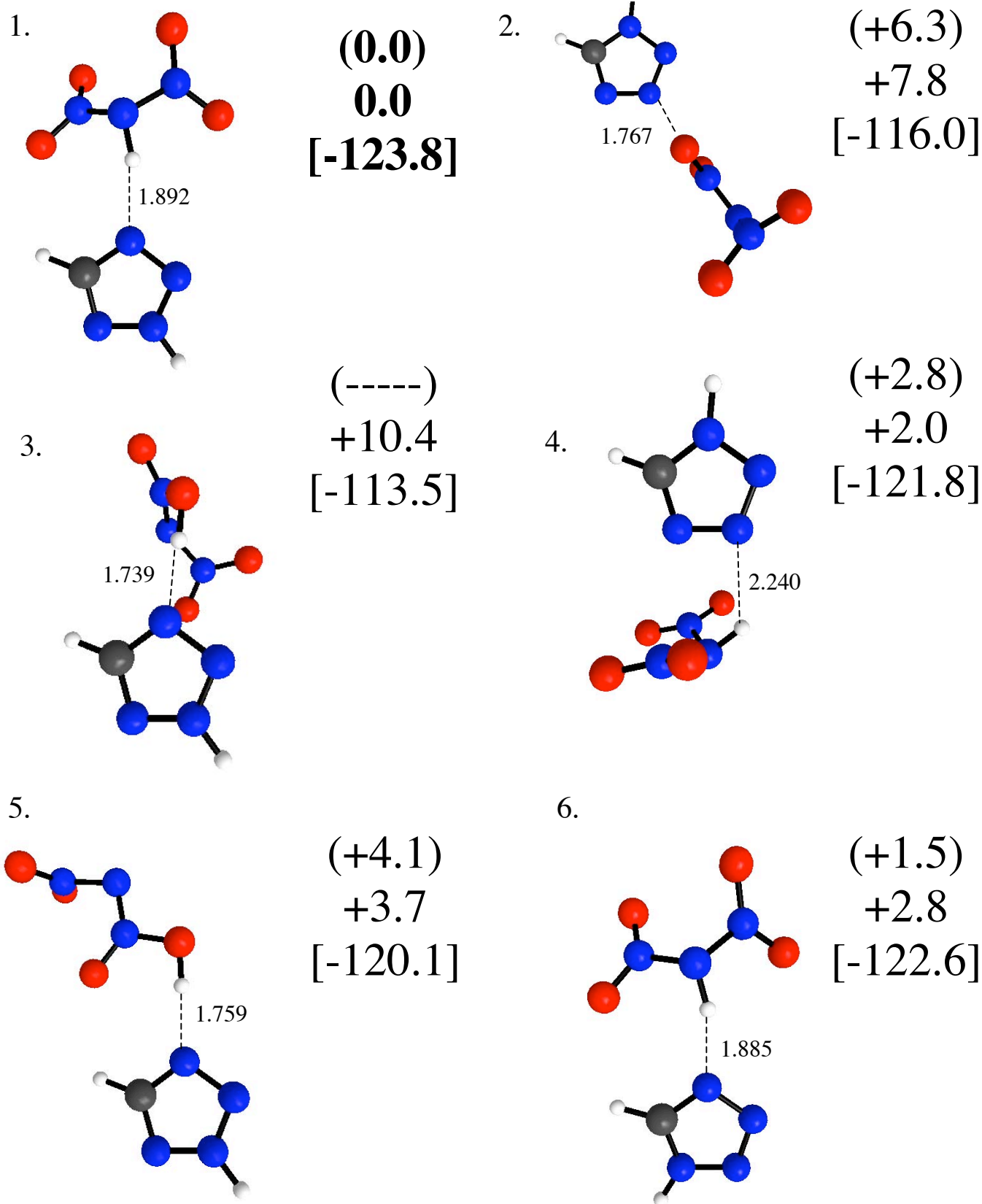
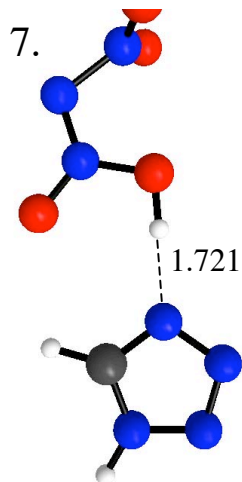
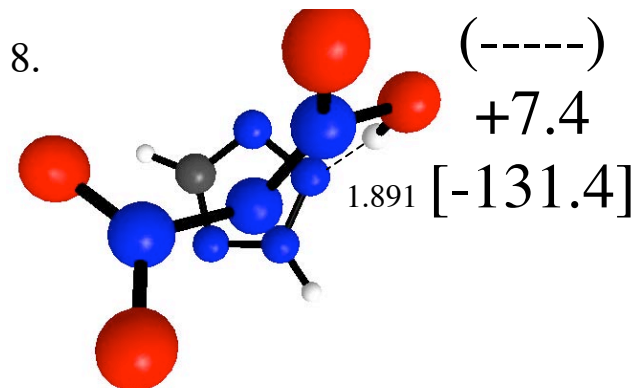


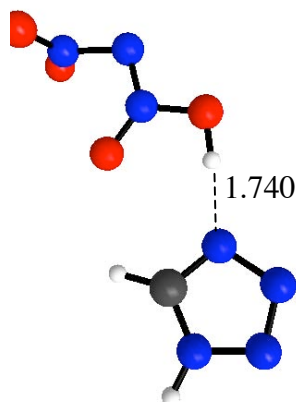
Figure 11: Optimized structures (Å) and MP2 and B3LYP (in parentheses) relative energies (kcal/mol) of the tetrazolium cation paired with a  $\text{N}(\text{NO}_2)_2^-$  anion. MP2 heats of reaction (in brackets) in kcal/mol for the reaction:  $\text{Tetrazolium} + \text{N}(\text{NO}_2)_2^- \rightarrow [\text{Tetrazole}][\text{HN}(\text{NO}_2)_2]$  or (see text)  $[\text{Tetrazolium}][\text{N}(\text{NO}_2)_2]$ .



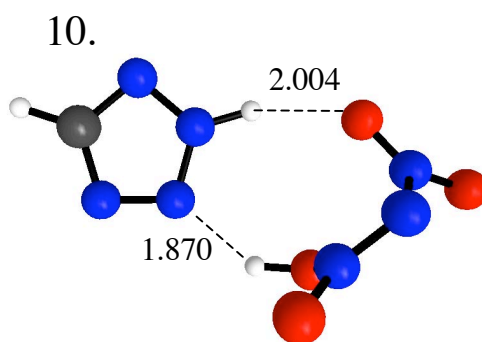
(+5.2)  
+8.1  
[-117.3]



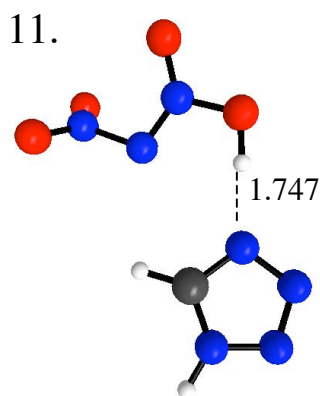
(-----)  
+7.4  
[-131.4]



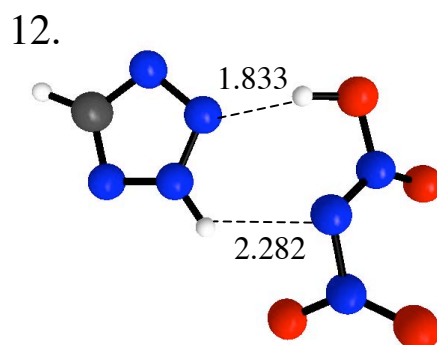
(+3.8)  
+6.0  
[-119.3]



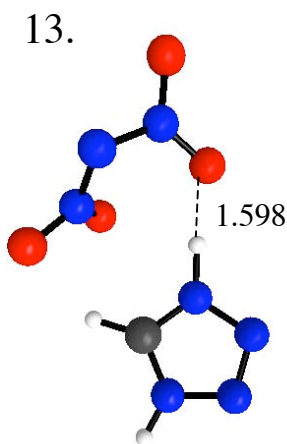
(+8.2)  
+7.5  
[-126.4]



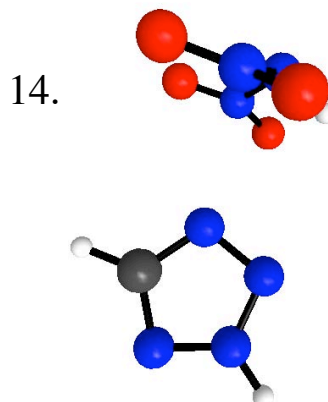
(+8.5)  
+6.7  
[-118.6]



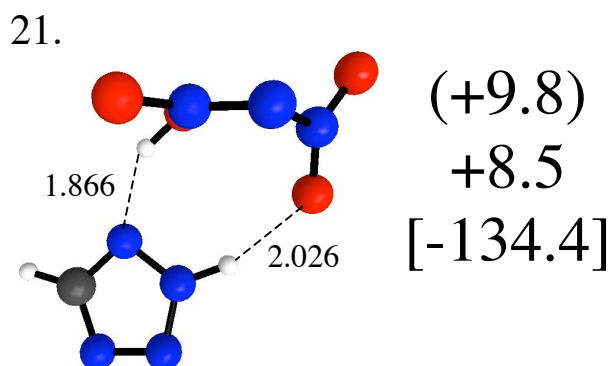
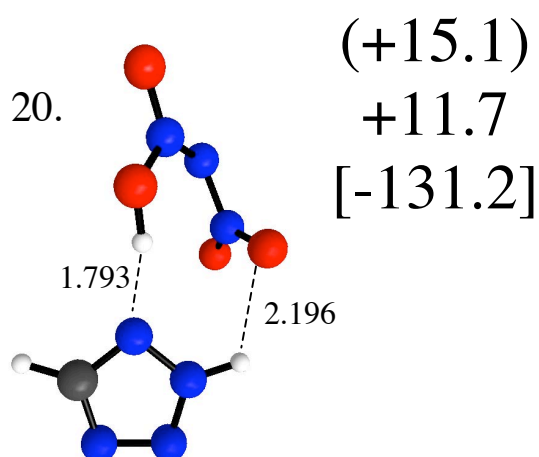
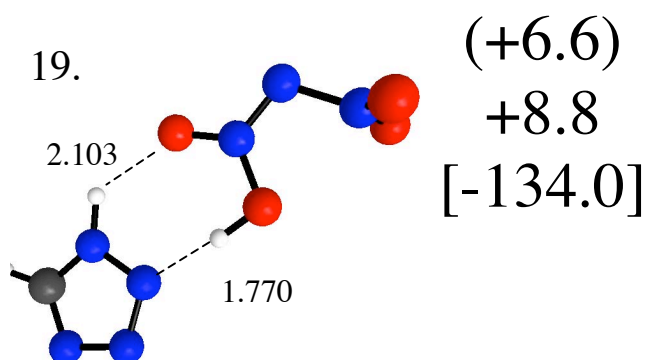
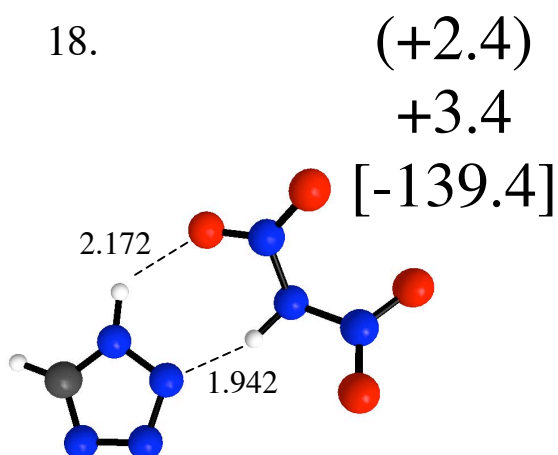
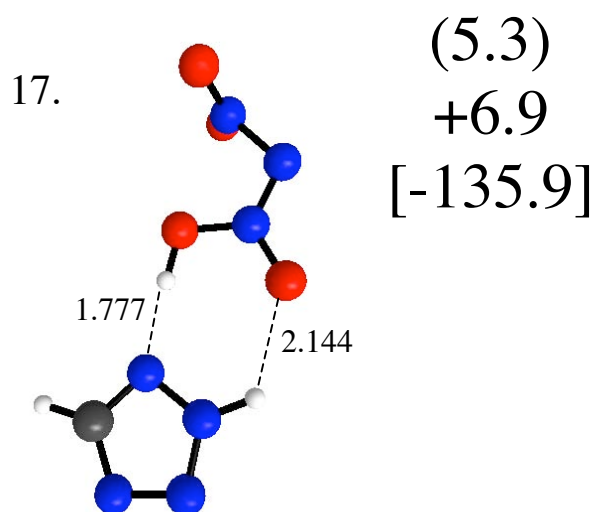
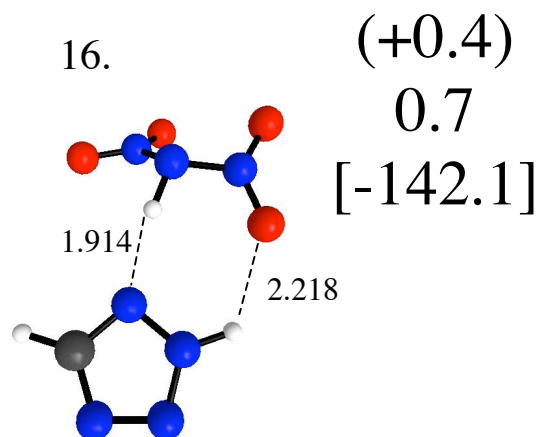
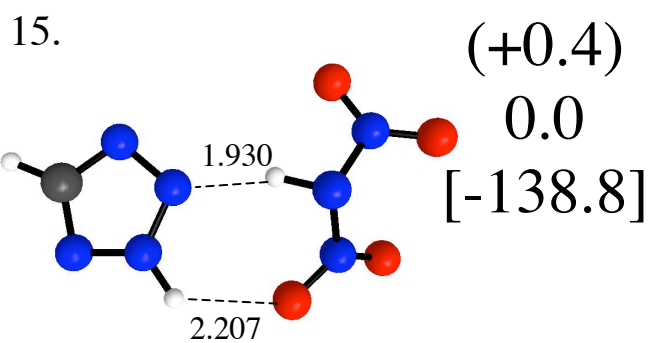
(+4.4)  
+4.5  
[-134.3]



(+13.1)  
+17.8  
[-106.4]



(-----)  
+0.1  
[-138.6]



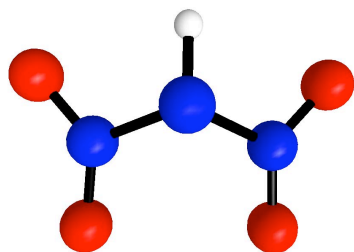
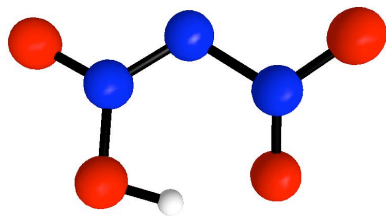
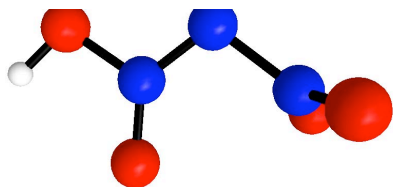


Figure 12: Three different geometries of dinitramic acid.

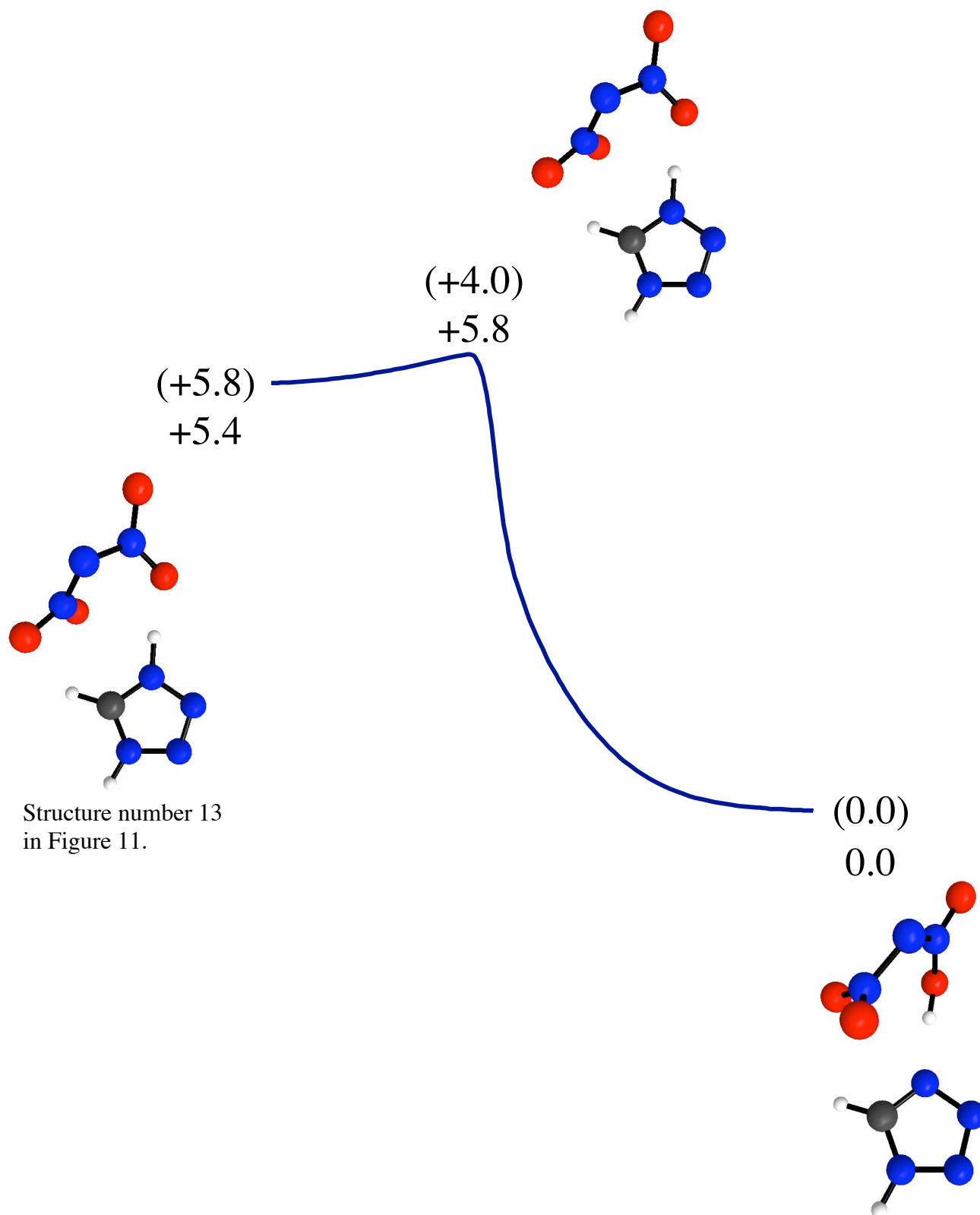


Figure 13: The MP2/6-31+G(d) potential energy surface for proton transfer from the 1,4,5-tetrazolium cation to the dinitramide anion to form 1,5-tetrazole and dinitramic acid. The relative energies including ZPE corrections are in parenthesis. Relative energies in kcal/mol.